Supplementary Information

Molecular Basis for Enantioselective Herbicide Degradation Imparted by Aryloxyalkanoate Dioxygenases (AADs) in Transgenic Plants

Jonathan R. Chekan[1,2,#], Chayanid Ongpipattanakul[1,#], Terry R. Wright[3], Bo Zhang[4], J. Martin Bollinger, Jr.[4,5], Lauren J. Rajakovich[4], Carsten Krebs[4,5], Robert M. Cicchillo[3],and Satish K. Nair[1,2,6,*]

[1]Department of Biochemistry, [2]Carl R. Woese Institute for Genomic Biology, and [6]Center for Biophysics and Quantitative Biology; University of Illinois, 600 S Mathews Ave, Urbana, IL, 61801, USA
and
[3]Corteva Agriscience™, Agriculture Division of DowDuPont, 9330 Zionsville Road, Indianapolis, IN, 46268, USA
and
[4]Department of Chemistry and [5]Department of Biochemistry and Molecular Biology, The Pennsylvania State University, University Park, Pennsylvania 16802

# These authors contributed equally to this work
Authors to whom correspondence should be addressed: snair@illinois.edu

TABLE OF CONTENTS

Supplementary Materials and Methods

General Procedures, Chemicals, and Reagents

All chemical reagents were purchased from Sigma-Aldrich unless otherwise noted. All of the material used for protein production and purification were purchased from GE Healthcare. *Escherichia coli* DH5α and BL21(DE3)Rosetta (Invitrogen) strains were used for plasmid maintenance and protein overexpression respectively unless otherwise noted.

Preparation of AAD-1 for Crystallographic Studies

Lyophilized AAD-1 supplied by Corteva Agriscience was resuspended in a buffer composed of 100 mM KCl and 20 mM HEPES free acid (pH 7.5) and further purified by size exclusion chromatography using a Superdex S75-16/60 column (GE Healthcare Life Sciences) equilibrated with the same buffer. Pure fractions were collected and concentrated to 50-60 mg/mL before storage in liquid nitrogen.

Cloning, Expression and Purification of AAD-2

The *aad2* gene from *Bradyrhizobium diazoefficiens* USDA 110 cloned into a pET28-a vector using the primer listed in **Supplementary Table S2**, and the resultant plasmid was transformed into *E. coli* containing the Rosetta plasmid for subsequent expression. AAD-2 was produced by growing the cells in shaking flask of LB media at a temperature of 37 $^{\circ}$C. When the cells reached an O.D.$_{600}$ of 0.6, the cells were cooled on ice for 15 minutes. Following the addition of 0.5 mM IPTG, the cells were placed in an 18 $^{\circ}$C shaking incubator for 18 hours. The cells were then harvested by centrifugation and resuspended in a buffer composed of 500 mM NaCl, 20 mM Tris base (pH 8.0), and 10% glycerol. Resuspended cells were lysed by sonication and the lysate was centrifuged at 14,000 rpm to remove cell debris. The cleared cell lysate was loaded onto a HisTrap column, which was subsequently washed with 1 M NaCl, 30 mM imidazole, and 20 mM Tris base (pH 8.0). Polyhistidine tagged AAD-2 was eluted using a linear gradient beginning with 1 M NaCl, 20 mM Tris base (pH 8.0), and 30 mM imidazole and ending with 250 mM imidazole. Pure fractions, as judged by SDS-PAGE, were combined and treated with thrombin (final ratio of 1:100 (w/w)) for 18 hours at 4 $^{\circ}$C to cleave the N-terminal tag. Tag-free AAD-2 was concentrated and loaded onto a size exclusion column (Superdex S75 16/60) pre-equilibrated with containing 100 mM KCl and 20 mM HEPES free acid (pH 7.5). Pure fractions were collected and concentrated to 25 mg/mL before storage in liquid nitrogen.

AAD-1 Activity under Conditions of Stopped-Flow and Freeze-Quench Experiments.

The stopped-flow absorption and freeze-quenched Mössbauer experiments were carried out essentially as previously described (1). The stopped-flow experiments were carried out at 5 °C on an Applied

Photophysics (Leatherhead, U.K.) SX20 instrument housed in a Labmaster MBraun glovebox. The instrument was configured for single mixing with an optical path length of 1 cm and detection with a photodiode-array (PDA). In the experiments shown in Figure 3A, an air-saturated buffer solution (50 mM sodium MOPS, pH 7.5, 10% glycerol) was mixed with an equal volume of an anoxic solution containing 1.1 mM AAD-1, 1.0 mM Fe(II), 10 mM αKG and either no primary substrate, 9 mM 2,4,-D, or 9 mM d_2-2,4-D. Owing to the complexity of the kinetic traces, no attempt was made to fit the data globally according to a necessarily elaborate kinetic model. Rather, traces were fit as the sum of exponentials to provide estimates for the observed rate constants characterizing the multiple phases of the reactions with and without the 2,4-D primary substrate (or its deuterium-containing isotopologue). In the freeze-quench Mössbauer experiment shown in Figure 3B, the reactant complex contained 2.2 mM AAD-1, 2.0 mM $^{57}Fe^{2+}$, 10 mM αKG, and 9.0 mM d_2-2,4D. It was mixed at 5 °C with an equal volume of O_2-saturated buffer (the same buffer used in the stopped-flow experiments), and the reaction was quenched by rapid freezing after 0.09 s. A second sample was quenched at a reaction time of 0.28 s to verify the transient nature of the new species detected in the 0.09-s sample. Mössbauer spectra were recorded on a constant acceleration Mössbauer spectrometer from Seeco (Edina, MN) equipped with a Janis SVT-400 variable temperature cryostat. Isomer shifts are reported with respect to the centroid of the spectrum of α-iron metal at room temperature. Simulations of Mössbauer spectra were carried out with the program WMOSS (Seeco, Edina, MN).

Determination of Substrate Scope and Kinetic Parameters

To determine the substrate scope for AAD-2, we used a coupled continuous assay monitoring the decrease in absorbance of NADH at 340nm using reactions in a 96-well microplate format. Reactions contained a total volume of 150 μL, with the following composition: 20 mM MOPS (pH 7.0), 200 μM $FeSO_4 \bullet 7H_20$, 200 μM L-ascorbic acid, 10μM AAD-2, 3 mM of each respective substrate, 14 units of lactate dehydrogenase (Roche), and 400 μM NADH. Assays were initiated by the addition of α-ketoglutarate to a final concentration of 1 mM. Plates were read using an Epoch Microplate Spectrophotometer (BioTek$^®$) and monitored using the Gen5 software (BioTek$^®$). Reactions were carried out in triplicate. Relative V_{max} over a linear range was determined for each substrate, and then the data was normalized against the highest relative V_{max}. Prism5 (GraphPad) was used to visualize the data.

To obtain kinetic parameters for AAD-2, an end point assay monitoring the emergence of a red quinone dye at 510 nm was utilized. Reactions contained 10 μM AAD-2, the appropriate volume of each serially diluted substrate, in the following buffer: 20 mM MOPS (pH 7.0), 200 μM $FeSO_4 \bullet 7H_20$, 200 μM L-ascorbic acid. Reactions were initiated in the same manner as aforementioned. All reactions were carried

out under ambient conditions: the system may have not necessarily been saturated in O_2. After the fifteen minutes, reactions were quenched with the addition of 10 μL of 100 mM EDTA (pH 8.0). To develop each reaction for absorbance readings at 510 nm, 15 μL of pH 10 buffer (3.09 g boric acid, 3.73 g KCl, 44 mL of 1N KOH), 0.2% 4-aminoantipyrine, and 0.8% potassium ferricyanide was added to each well. The resultant color was allowed to develop for three minutes before absorbance readings were performed. Additional kinetic parameters for AAD-1 were obtained using the same experimental procedures as for AAD-2, except that only 2 μM of enzyme was used. Reactions were carried out in triplicate; Prism5 (GraphPad) was used to analyze and visualize the data.

Crystallization of AAD-1 and AAD-2

Preliminary crystals of AAD-1 in complex with Mn^{2+}, αKG, and (*R*)-dichlorprop were obtained using a sparse matrix screen. Diffraction quality crystals were grown using hanging drop vapor diffusion with 8 mg/mL AAD-1 pre-incubated with 5 mM (*R*)-dichlorprop, 5 mM αKG, and 5 mM $MnCl_2$. The protein mixture was added to mother liquor containing 25% PEG 3350, 0.3 M Li_2SO_4, and 0.1 M bicine (pH 9.0) in a 1:1 ratio at 4 °C. Crystals of AAD-1 in complex with (*R*)-cyhalofop or (*R*)-diclofop were obtained in a similar manner. Diffraction quality crystals of AAD-1 (10-15 mg/mL) in complex with (*R*)-dichlorprop (5 mM), and vanadyl sulfate (1 mM) were obtained by seeding using the same conditions described above. Addition of succinate in the drop impeded crystallization, and complexes were obtained by soaking crystals of AAD-1/vanadyl/(*R*)-dichlorprop in crystallization media supplemented with 5 mM succinate. Crystals of AAD-2 in complex with Mn^{2+} and NOG were first observed using a sparse matrix screen and refined using the hanging drop method. Briefly, AAD-2 (8-12 mg/mL), was incubated with (*S*)-dichlorprop, Mn^{2+}, and NOG (each at 2 mM) for 20 minutes and then mixed with a solution containing 22-28% PEG 4000, 0.07 M $LiSO_4$, and 0.1 M MES (pH 6.0) and equilibrated against the same solution. Crystals of all samples were briefly soaked in mother liquor supplemented with either 15% glycerol (AAD-1) or 15% ethylene glycol (AAD-2) immediately prior to vitrification by direct immersion into liquid nitrogen.

Bioinformatics

The sequence divergence of known AAD members limited identification of other AADs based solely on sequence similarities with select members of PF20668 (TauD) superfamily. Thus, the sequences of TfdA, AAD-1, and AAD-12 were each used to generate Sequence Similarity Networks (SSNs) (2) based on individual BLAST search (1000 sequences each). Gene Neighborhood Networks (GNNs) (3), using a gene window of 15 genes upstream and downstream of each sequence node, were then constructed for each SSN output. Each graphical GNN was then examined for presence for the following PFAMs:

PF01494 (TfdB-like monooxygenases), or PF00775 fused to PF04444 (TfdC-like 1, 2 catechol dioxygenases). Clusters that contain mis-annotated PF01494, and PF00775 and PF04444 were included. Clusters that contained PF00775 fused to PF12391 (protocatechuate 3, 4-dioxygenases) were also included. The final SSN was generated using these sequences, along with sequences of TfdA, AAD-1, AAD-12, and 238 randomly selected members of the TauD superfamily (1/170 of all annotated TauD family members in the Uniref90 database). A representative node network at sequence similarity of 100% was used in order to filter through duplicate entries that were obtained during the initial query. Singletons (i.e. nodes with no other similar sequences) were omitted from Fig. 2 to concisely visualize the data.

Cupriavidus necator (strain JMP 134)

TfdA (α-KG dependent dioxygenase)
TfdB (2, 4-dichlorophenol 6-monooxygenase)
TfdC (chlorocatechol 1, 2-dioxygenase)
TfdD (chloromuconate cycloisomerase)
TfdE (carboxymethylenebutenolidase)
TfdF (maleylacetate reductase)
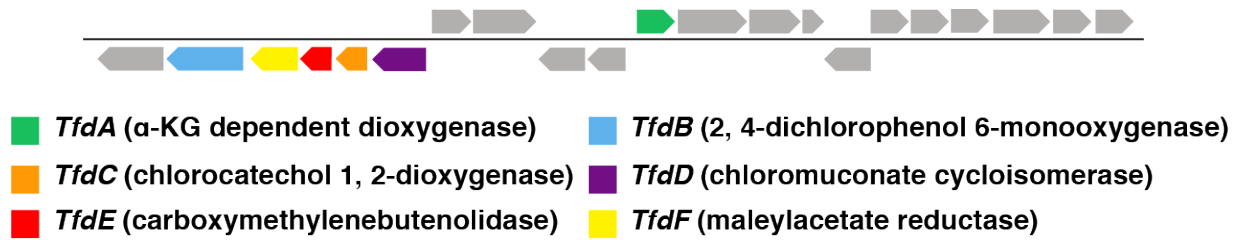
Supplementary Figure 1. Genomic context of *Tfd*A-F from the conjugative plasmid pJP4. Plasmid pJP4 was initially detected in the host bacterium *Cupriavidus necator* JMP134 (4). Genes of importance to degradation pathways are highlighted and annotated according to the legend below. Proteins that are non-essential to the pathway have been colored grey.
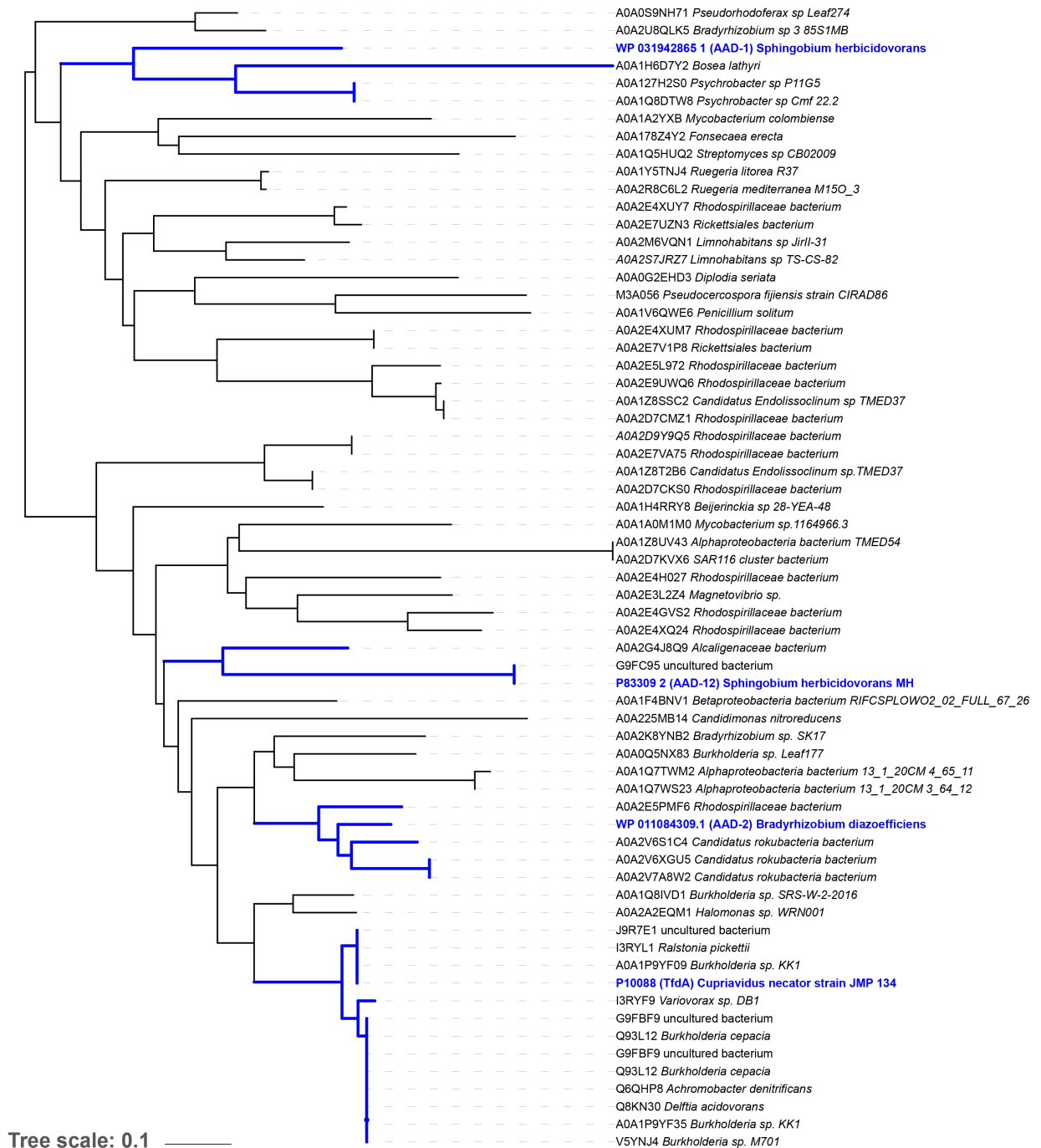
Supplementary Figure 2. Phylogenetic tree of putative AAD sequences. Sequences manually culled and used for the SNN/GNN analysis are shown in black, while sequences in blue are AADs of interest that have been biochemically characterized. Clades that contain the AADs of interest are also noted in blue.

Sphingobium herbicidovorans strain MH plasmid pMSHV

■ AAD-1   **■** TfdB (2, 4-dichlorophenol 6-monooxygenase)   **■** TfdC (chlorocatechol 1, 2-dioxygenase)

■ TfdF (maleylacetate reductase)   **■** Carboxymucolactone decarboxylase

Delftia acidovorans (plasmid pMC1)

■ AAD-12 (SdpA)   **■** RdpA   **■** TfdC (chlorocatechol 1, 2-dioxygenase)

■ TfdD (chloromuconate cycloisomerase)   **■** Carboxymucolactone decarboxylase
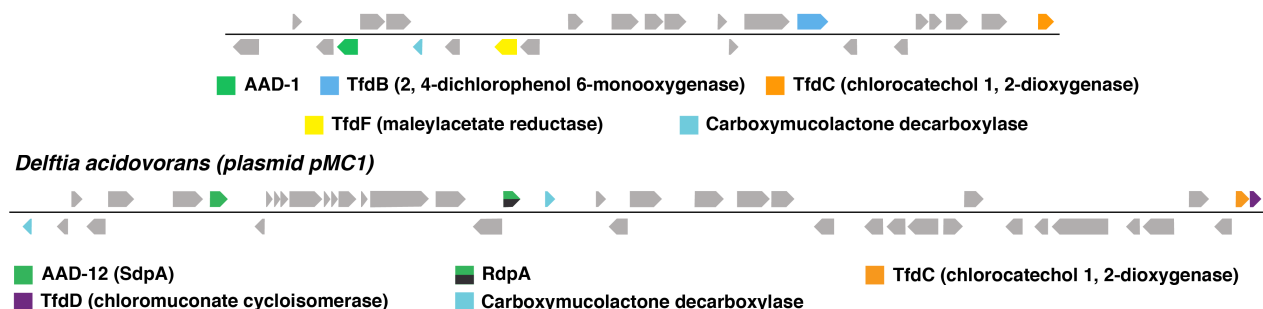
Supplementary Figure 3. Genomic context of AAD-1 and AAD-12. The genomic context highlights the distal nature of potential biosynthetic genes. We note that the genomic context of AAD-1 is that of a homolog (98% amino acid sequence similarity to the AAD-1 that was crystalized), as there is no annotated genomic data for corresponding organism and conjugative plasmid in public databases. Annotated genomic context of AAD-2 was also not available in public databases. Genes of importance to degradation pathways are highlighted and annotated according to the legend below. Proteins that are non-essential to the pathway have been colored grey.
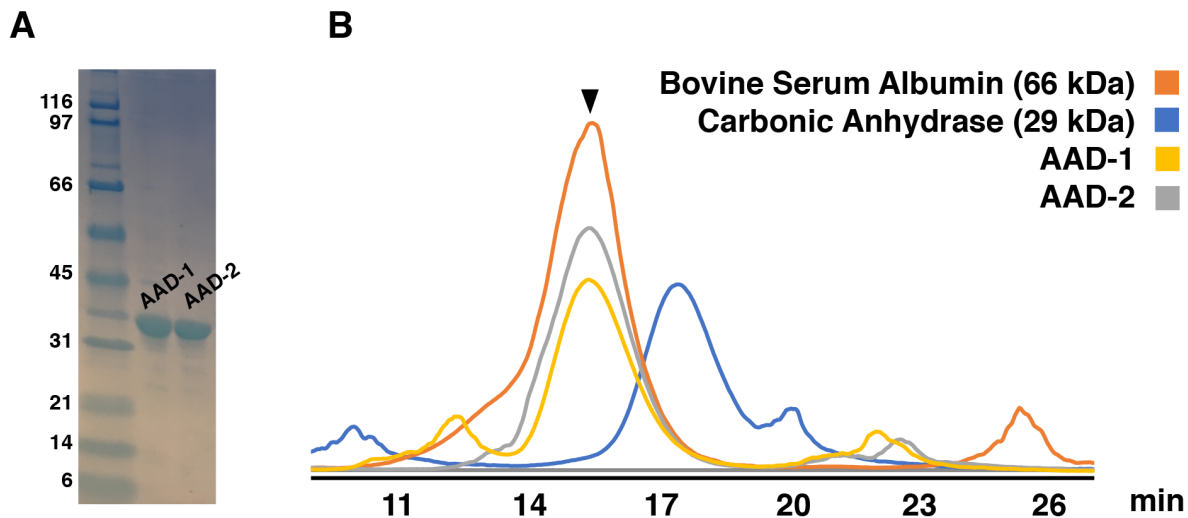
Supplementary Figure 4. Analytical Gel Filtration and SDS-PAGE analysis of AADs. (A) SDS-PAGE gel of AAD-1 and AAD-2 used for crystallographic and biochemical studies. (B) Analytical gel filtration of AAD-1 (33.2 kDa) and AAD-2 (33.6 kDa) against known standards. Elution profile suggests that AAD-1 and AAD-2 assemble as dimers in solution, denoted by the black arrow at ~15 min elution.
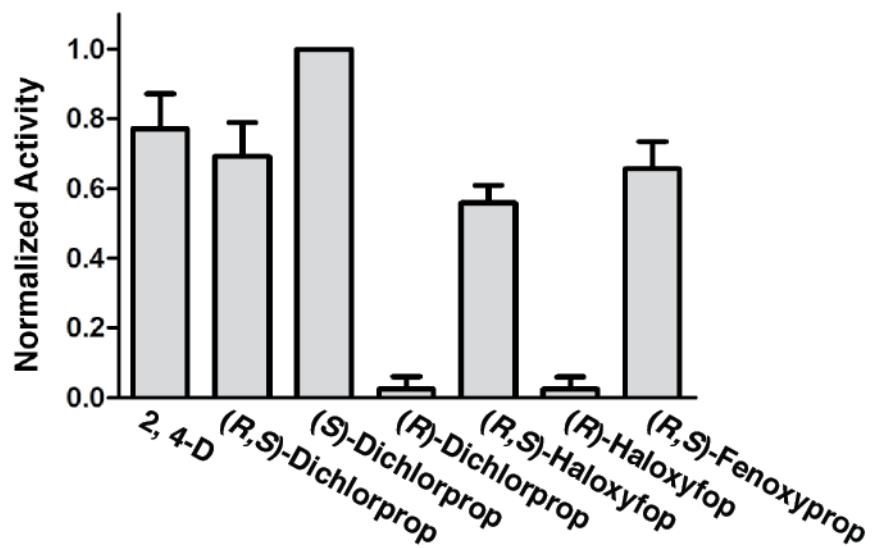
Supplementary Figure 5. Normalized activity of AAD-2 against a panel of substrates. The activity reported has been normalized to the activity of AAD-2 against (*S*)-dichlorprop, which was the substrate it most preferred amongst those tested.
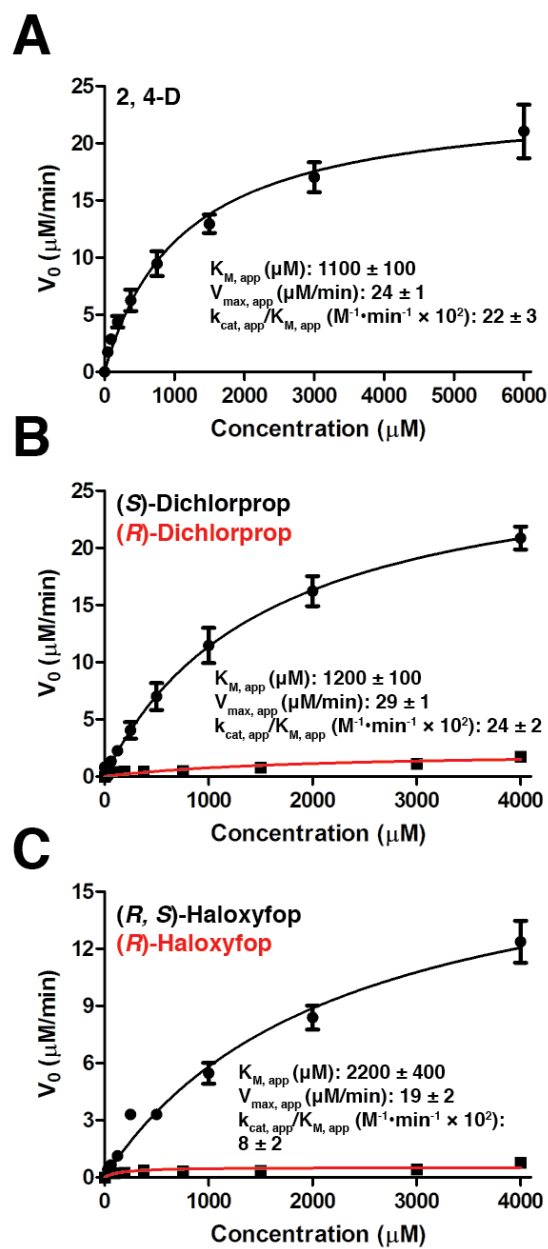
Supplementary Figure 6. Kinetic curves for the AAD-2 reaction using various substrates. (A) Kinetic curve of AAD-2 with 2,4-D at various concentrations. (B) Kinetic curves of AAD-2 with (*S*)-dichlorprop (black curve) or (*R*)-dichlorprop (red curve). (C) Kinetic curves of AAD-2 with (*R,S*)-haloxyfop (black curve) or (*R*)-haloxyfop (red curve). For racemic substrates, the concentration noted is the effective concentration of the (*S*) enantiomer in the sample. Kinetic parameters noted in each pane l correspond to values calculated using the black curve in each panel.
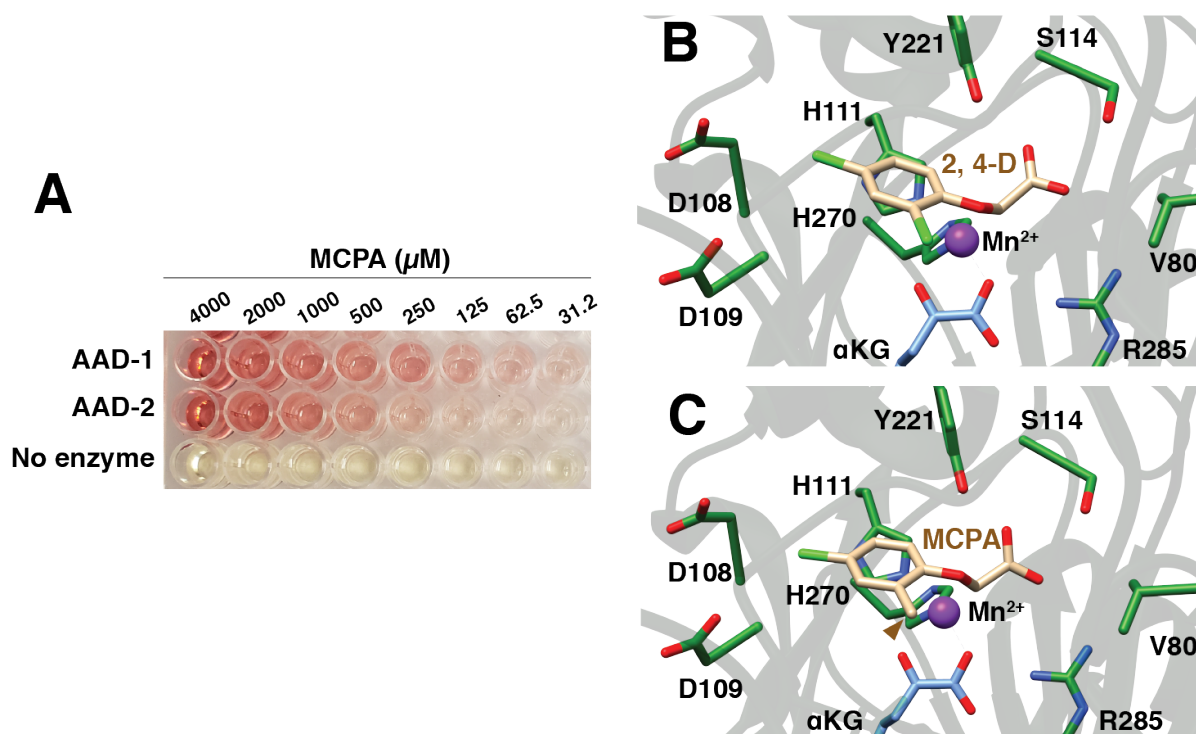
Supplementary Figure 7. AAD-1 and AAD-2 can accept MCPA as a substrate. (A) Select wells in a 96-well plate depicting the characteristic red color indicative of the presence of a phenol product (developed under basic conditions using 4-aminoantipyrine and potassium ferricyanate) as AAD-1 and AAD-2 react with MCPA at varying concentrations. The no enzyme control lane has been included to show that a null reaction will produce a pale yellow color. (B) Docking model depicting 2,4-D in the active site of AAD-1. (C) Docking model depicting MCPA in the active site of AAD-1. MCPA differs from 2,4-D only by the presence of a methyl group (brown arrow). AAD-1 was chosen to model in the achiral substrates as the structure of AAD-2 does not contain electron density for a herbicide substrate.

.
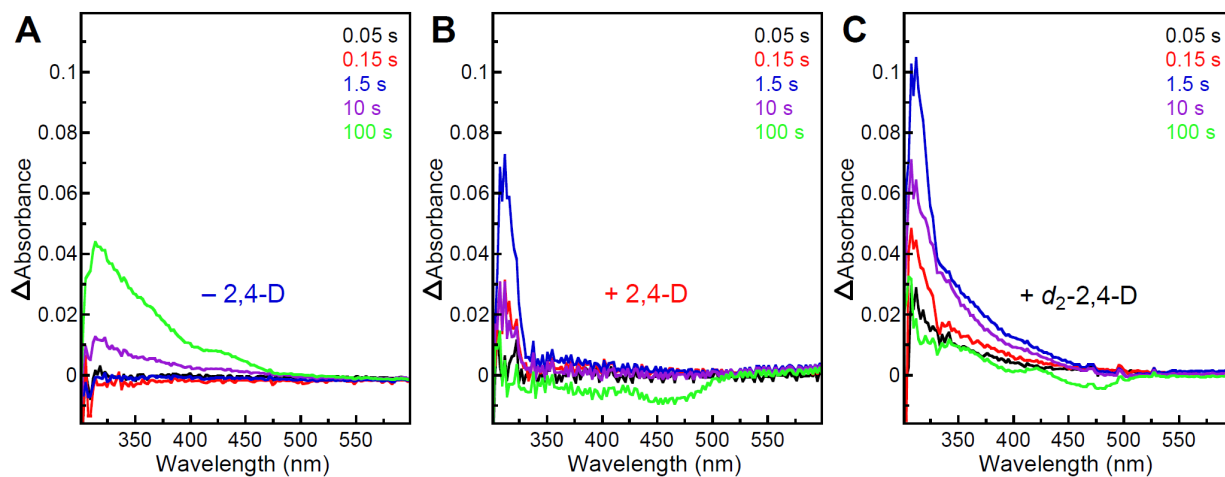
Supplementary Figure 8. Kinetic-difference spectra from the stopped-flow absorption experiment. The spectra shown here are the results of subtracting the experimental spectrum of an early reaction time (0.005 s) from the spectra taken at the reaction times indicated in the legend in the experiments with (A) no primary substrate, (B) unlabeled 2,4-D, and (C) d_2-2,4-D. The reaction conditions are given in Supplemental Materials and Methods.
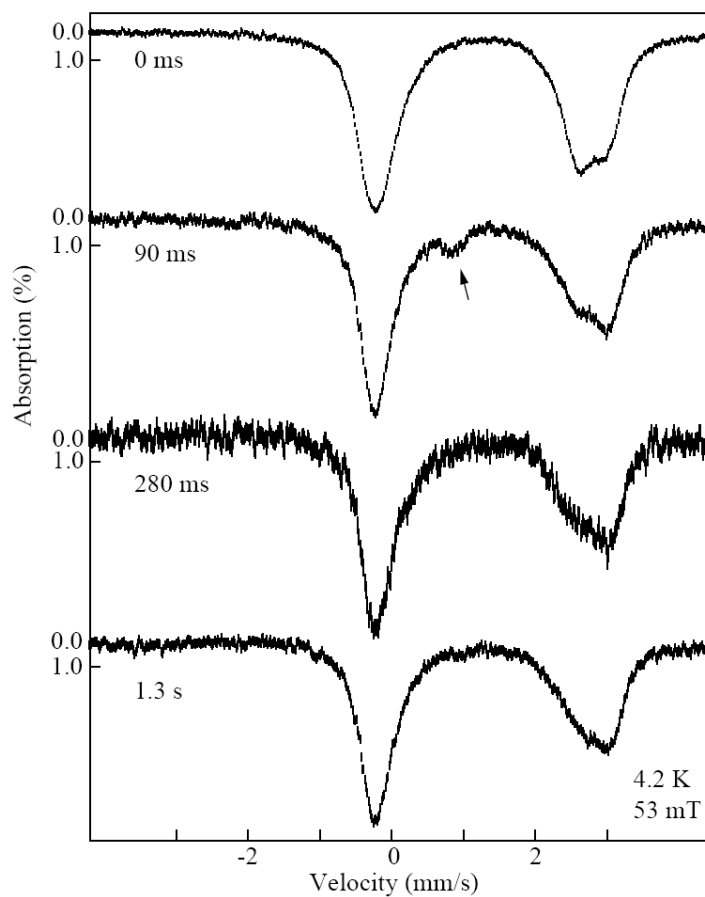
Supplementary Figure 9. Mössbauer spectra of samples of the AAD-1 reaction. 4.2-K/53-mT Mössbauer spectra of a sample of the AAD-1•Fe(II) •αKG•d_2-2,4-D reactant complex (top) and samples, wherein the reactant complex was reacted for 90 ms, 280 ms, or 1.3 s. The position of the high-energy line of the ferryl intermediate is indicated with an arrow in the spectrum of the 90-ms sample. The reaction conditions are given in Supplemental Materials and Methods.
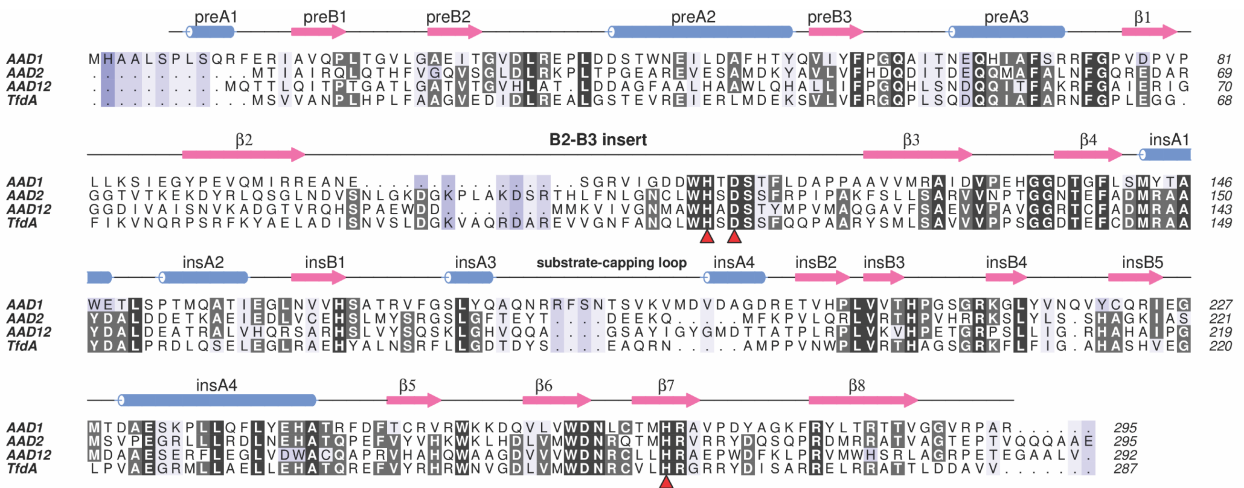
Supplementary Figure 10. Sequence alignment of select AADs. Sequence alignment of select AADs, noting secondary structure elements, and the β2β3 insert found in AAD-12 and AAD-2.

	Organism	Uniprot ID
Co-localizes with TfdB-like protein	Pseudocercospora fijiensis (strain CIRAD86)	M3A056
	Penicillium solitum	A0A1V6QWE6
	Fonsecaea erecta	A0A178Z4Y2
	Mycobacterium colombiense	A0A1A2YXB1
	Streptomyces sp. CB02009	A0A1Q5HUQ2
	Mycobacterium sp. 1164966.3	A0A1A0M1M0
	Alphaproteobacteria bacterium TMED54	A0A1Z8UV43
	SAR116 cluster bacterium	A0A2D7KVX6
	Rhodospirillaceae bacterium	A0A2D9Y9Q5
	Rhodospirillaceae bacterium	A0A2E7VA75
	Candidatus Endolissoclinum sp. TMED37	A0A1Z8T2B6
	Rhodospirillaceae bacterium	A0A2D7CKS0
	Rhodospirillaceae bacterium	A0A2E4GVS2
	Rhodospirillaceae bacterium	A0A2E4XQ24
	Magnetovibrio sp.	A0A2E3L2Z4
	Rhodospirillaceae bacterium	A0A2E4H027
	Alphaproteobacteria bacterium 13_1_20CM_4_65_11	A0A1Q7TWM2
	Alphaproteobacteria bacterium 13_1_20CM_3_64_12	A0A1Q7WS23
	Betaproteobacteria bacterium RIFCSPLOWO2_02_FULL_67_26	A0A1F4BNV1
	Alcaligenaceae bacterium	A0A2G4J8Q9
	Rhodospirillaceae bacterium	A0A2E5PMF6
	Candidatus Rokubacteria bacterium	A0A2V6XGU5
	Candidatus Rokubacteria bacterium	A0A2V7A8W2
	Burkholderia sp. SRS-W-2-2016	A0A1Q8IVD1
Co-localizes with TfdC-like protein	Diplodia seriata	A0A0G2EHD3
	Candidatus rokubacteria bacterium	A0A2V6S1C4
	Burkholderia sp. Leaf177	A0A0Q5NX83
	Bradyrhizobium sp. SK17	A0A2K8YNB2
	Halomonas sp. WRN001	A0A2A2EQM1
	Burkholderia sp. KK1	A0A1P9YF09
	Rhodospirillaceae bacterium	A0A2E4XUY7
	Rickettsiales bacterium	A0A2E7UZN3
	Rhodospirillaceae bacterium	A0A2E4XUM7
	Rickettsiales bacterium	A0A2E7V1P8

	Organism	UniprotID
Co-localizes with TfdC-like protein	Candidatus endolissoclinum sp. TMED37	A0A1Z8SSC2
	Rhodospirillaceae bacterium	A0A2D7CMZ1
	Rhodospirillaceae bacterium	A0A2E9UWQ6
	Rhodospirillaceae bacterium	A0A2E5L972
	Pseudorhodoferax sp. Leaf274	A0A0S9NH71
	Bradyrhizobium sp. 3 85S1MB	A0A2U8QLK5
	Bosea lathyri	A0A1H6D7Y2
	Beijerinckia sp. 28-YEA-48	A0A1H4RRY8
	Uncultured bacterium	G9FC95
Co-localizes with TfdB and TfdC-like proteins	uncultured bacterium	G9FBF9
	Burkholderia cepacia	Q93L12
	Achromobacter denitrificans	Q6QHP8
	Uncultured bacterium	G9FBF9
	Burkholderia cepacia	Q93L12
	Achromobacter denitrificans	Q6QHP8
	Delftia acidovorans	Q8KN30
	Burkholderia sp. KK1	A0A1P9YF35
	Burkholderia sp. M701	V5YNJ4
	Ralstonia pickettii	I3RYL1
	Uncultured bacterium	J9R7E1
	Variovorax sp. DB1	I3RYF9
	andidimonas nitroreducens	A0A225MB14
	Psychrobacter sp. P11G5	A0A127H2S0
	Psychrobacter sp. Cmf 22.2	A0A1Q8DTW8
	Ruegeria litorea R37	A0A1Y5TNJ4
	Ruegeria mediterranea M15O_3	A0A2R8C6L2
	Limnohabitans sp. JirII-31	A0A2M6VQN1
	Limnohabitans sp. TS-CS-82	A0A2S7JRZ7

Supplementary Table 1. List of Uniprot IDs of Putative AADs Identified by EFI-EST (2). The table above lists the UniprotIDs of putative AADs found using the EFI-FEST Sequence Similarity Network (SSN) and Genome Neighborhood Network (GNN) tools (3). Sequences are group to whether they co-occur (within a 15 gene window) with a TfdB homolog, TfdC homolog, or both.

Substrate	AAD-1		AAD-2	
	$K_{M,\ app}$ (μM)	$k_{cat,\ app}/K_{M,\ app}$ ($M^{-1}\cdot min^{-1} \times 10^3$)	$K_{M,\ app}$ (μM)	$k_{cat,\ app}/K_{M,\ app}$ ($M^{-1}\cdot min^{-1} \times 10^2$)
2, 4-D	683 ± 76*	27*	1100 ± 100	22 ± 3
(R)-dichlorprop	527 ± 38*	3380*	N. D.	N. D.
(S)-dichlorprop	N. D.	N. D.	1200 ± 100	24 ± 2
(R)-cyhalofop	96 ± 7*	1950*	N. D.	N.D.
(R,S)-diclofop	160 ± 40	97 ± 5	N. S.	N.A.
(R,S)-haloxyfop	330 ± 100	50 ± 2	2200 ± 300	8 ± 2
(R,S)-quizalofop	120 ±30	32 ± 3	N.S.	N.A

Supplementary Table 2. Kinetic parameters of AAD-1 and AAD-2 across a panel of substrates. Values denoted with an * were previously reported (5). The aforementioned values have been converted from $M^{-1}\cdot s^{-1} \times 10^3$ as reported, to $M^{-1}\cdot min^{-1} \times 10^3$ to provide a more direct means of comparison. Values noted with N. D. (not detected) indicate that the no activity was detected. Values noted with N. S. (not saturated) suggests that the enzyme does not prefer that compound as a substrate, i.e. only a subtle colorimetric change at 510nm was observed when 10 μM of enzyme was incubated with 4mM (effective concentration) of the accepted enantiomer of over a 15 minute incubation period. The lack in change of absorbance hindered our kinetic assays due to issues in detection. Unless otherwise noted, all other values were obtained during this study.

Primer	Sequence
AAD-2_NLIC_FP	TACTTCCAATCCAATGCAATGACGATCGCCATCCGGCAGCTT
AAD-2_NLIC_RP	TTATCCACTTCCAATGTTATTATCACTCCGCCGCCTGCTGCTG

Supplementary Table 3. List of primers used in this study.

Supplementary Table 3. Data collection, phasing and refinement statistics

	AAD-1 $Mn^{2+} \cdot \alpha KG \cdot$ (R)-dichlorprop	AAD-1 $Mn^{2+} \cdot \alpha KG \cdot$ (R)-dicyhalofop	AAD-1 $Mn^{2+} \cdot \alpha KG \cdot$ (R)-diclofop	AAD-1 $(VO)^{2+} \cdot succ \cdot$ (R)-dichlorprop	AAD-2 $Mn^{2+} \cdot \alpha KG$
Data collection					
Space group	$P2_12_12$	$P2_12_12$	$P2_12_12$	$P2_12_12$	C2
Unit cell	85.9, 97.8, 69.9	85.5, 97.4, 69.8	85.8, 97.78, 69.9	85.9, 97.9, 69.9	266.5, 55.5, 183.7, 118.9°
Resolution	86-1.58 (1.59-1.58)	86-1.9 (1.91-1.9)	86-1.8 (1.81-1.8)	57-1.5 (1.54-1.5)	50-2.15 (2.19-2.15)
Total reflections	656,362	380,331	508,030	1,275,386	579,196
Unique	80,901	46,644	55,192	92,316	127,502
R_{sym} (%)[1]	0.093 (0.956)	0.119 (755)	0.111 (0.929)	0.072 (0.792)	0.088 (0.720)
$I/\sigma(I)$ [1]	17.5 (2.1)	17.0 (2.9)	18.7 (2.6)	20.5 (2.2)	16.1 (1.6)
Completeness	100 (95.8)	100 (97.7)	100 (97.3)	99.2 (99.4)	99.0 (92.6)
Redundancy	8.1 (7.9)	8.2 (8.3)	9.2 (9.3)	13.8 (8.2)	4.6 (3.8)
Refinement					
Resolution (Å)	54.2-1.58	56.7-1.9	48.9-1.8	25.0-1.51	25.0-2.15
# reflections	80,828	46,591	55,138	87,655	107,559
R_{work} / R_{free}[2]	16.2/19.7	17.5/21.8	16.3/20.1	19.5/21.7	18.8/23.3
# of atoms					
Protein	4,497	4,500	4,482	4,498	15,111
αKG/succinate	20	20	20	8	70
Herbicide	14	44	21	14	-
Water	734	576	668	650	1,633
B-factors					
Protein	19.4	21.5	19.6	22.0	34.7
αKG/succinate	14.6	17.5	15.5	22.8	34.1
Herbicide	22.1	32.9	32.6	38.2	-
Water	30.3	28.7	29.6	32.4	38.1
RMS deviations					
Bond lengths (Å)	0.011	0.004	0.007	0.007	0.009
Bond angles (°)	1.249	0.865	1.066	1.16	1.29

1. Highest resolution shell is shown in parenthesis.

2. R-factor = $\Sigma(|F_{obs}|-k|F_{calc}|)/\Sigma|F_{obs}|$ and R-free is the R value for a test set of reflections consisting of a random 5% of the diffraction data not used in refinement.

SUPPLEMENTAL REFERENCES

1.   Price JC, Barr EW, Hoffart LM, Krebs C, & Bollinger JM, Jr. (2005) Kinetic dissection of the catalytic mechanism of taurine:alpha-ketoglutarate dioxygenase (TauD) from *Escherichia coli*. *Biochemistry* 44:8138-8147.

2.   Gerlt JA*, et al.* (2015) Enzyme Function Initiative-Enzyme Similarity Tool (EFI-EST): A web tool for generating protein sequence similarity networks. *Biochim Biophys Acta* 1854:1019-1037.

3.   Gerlt JA (2017) Genomic Enzymology: Web tools for leveraging protein family sequence-function space and genome context to discover novel functions. *Biochemistry* 56:4293-4308.

4.   Don RH & Pemberton JM (1981) Properties of six pesticide degradation plasmids isolated from Alcaligenes paradoxus and Alcaligenes eutrophus. *J Bacteriol* 145:681-686.

5.   Wright TR*, et al.* (2010) Robust crop resistance to broadleaf and grass herbicides provided by aryloxyalkanoate dioxygenase transgenes. *Proc Natl Acad Sci U S A* 107:20240-20245.